Available online at www.sciencedirect.com
ScienceDirect
Journal of the European Ceramic Society 27 (2007) 623–628
www.elsevier.com/locate/jeurceramsoc

Devitrification behaviour of plasma-sprayed glass coatings

G. Bolelli, L. Lusvarghi *, T. Manfredini, C. Siligardi

Dipartimento di Ingegneria dei Materiali e dell'Ambiente (DIMA), Facoltà di Ingegneria, Università di Modena e Reggio Emilia, Via Vignolese 905, 41100 Modena, Italy

Available online 9 June 2006

Abstract

Glass and glass-ceramic coatings on ceramic tiles have been manufactured by plasma-spraying high-performance CAS (in wt%—SiO_2, 60%; Al_2O_3, 15%; CaO, 23%; others, traces) and CZS (in wt%—SiO_2, 50%; CaO, 31%; ZrO_2, 16.5%; Al_2O_3, 2%; others, traces) glass frits. The CZS system has a surface crystallization at about 1050 °C. Such behaviour would not easily allow to obtain a fully crystalline bulk glass-ceramic, but the defectiveness of the plasma-sprayed coating supplies many nucleation sites. Thus, it becomes completely crystalline and well sintered after a 850 °C for 30 min + 1050 °C for 15 min treatment. The CAS frit, designed not to produce significant crystallization, is well sintered after a 850 °C for 30 min + 950 °C for 30 min thermal treatment, but remains too brittle due to its glassy nature. A 1050 °C treatment allows a few pseudowollastonite crystals to form in a glassy matrix; their formation also hinders sintering. Thus, mechanical properties are inferior to heat-treated plasma-sprayed CZS.

Keywords: Plasma spraying; Toughness and toughening; Glass ceramics; Microstructure-final; Hardness

1. Introduction

Generally, glazing of ceramic substrates involve the dry or wet application of a powdered material onto a raw or fired substrate and subsequent firing of the substrate together with the glaze, in order to achieve sintering. Obviously, this processing technique imposes many limitations on the choice of glazing materials; in particular, the glaze must have the same firing temperature and same thermal expansion coefficient as the substrate, in order to properly sinter both and to prevent thermal residual stresses.[1] This means that high mechanical properties systems cannot be applied because they often have high melting points and high processing temperatures as well. Traditional ceramics are often coated with glassy or glass-ceramic glazes, due to their combination of adequate wear resistance and esthetical qualities; however, glasses or glass-ceramics with high mechanical strength also have high T_g, so that they must be mixed with low-melting-point compounds and low-T_g frits, reducing the overall glaze mechanical properties. Such troubles could be circumvented by thermal spraying techniques. They basically consist in feeding the coating material, as a powder or as a wire, in a hot gas jet, where it is melted and accelerated towards a substrate, which is kept at low or moderate temperature. The torch passes over the substrate several times, so that the coating consists in a superposition of layers made by flattened and solidified droplets (called splats or lamellae).[2,3] Repeated torch passes cause some thermal cycling to the previously-deposited coating layers. Among thermal spraying techniques, the plasma-spraying is probably the fittest to spray glass powders: the hot gas jet consists in a plasma flux, whose high temperature make it suitable for spraying ceramic materials in general.[4] However, plasma-spraying has seldom been tested with glasses, except for a few cases,[5–7] especially in the biomedical field.[8,9] Should a post-process thermal treatment on the sprayed coating be needed, the treatment temperature would be much lower than traditional firing processes, so that thermal expansion mismatch is definitely less important.

2. Experimental

Two industrially manufactured frits, which are commonly employed (in little amounts, due to the above mentioned firing troubles) as constituents of tile glazes, have been chosen. They belong to the CZS system (nominal composition (in wt%)—SiO_2, 50%; CaO, 31%; ZrO_2, 16.5%; Al_2O_3, 2%; others, traces; expressly designed for devetrification[10]), and to the

* Corresponding author. Tel.: +39 0592056206; fax: +39 0592056243.
E-mail address: lucalusv@unimore.it (L. Lusvarghi).

0955-2219/$ – see front matter © 2006 Elsevier Ltd. All rights reserved.
doi:10.1016/j.jeurceramsoc.2006.04.119

Table 1
Plasma torch operating parameters

Nozzle diameter	6 mm
Power	600 A × 72 V = 43.20 kW
Spraying distance	115 mm
Number of passes	3 pre-heating; 27 spraying
Carrier gas type and flow rate	Ar, 3 slpm
Plasma gas composition and flow rates	Ar, 50 slpm; H_2, 14 slpm
Cooling system	Ar at 7.5×10^5 Pa through two nozzles
Substrate temperature during deposition	80–140 °C

CAS one (nominal composition (in wt%)—SiO_2, 60%; Al_2O_3, 15%; CaO, 23%; others, traces), respectively. Spray powders with suitable particle size distribution were produced by wet ball milling (planetary-moving mill, 500 g of frit + 500 g of 25 mm diameter alumina balls + 300 g water in 1 l porcelain jars), simulating the conventional ceramic milling process. Powders were characterized by chemical analysis (ICP-AES, Liberty 200, Varian), differential thermal analysis (DSC 404, Netzsch), grain size distribution analysis (Particle Sizer Analysette 22, Fritsch), X-ray diffractometry (PW 3710, Philips, Cu Kα radiation). The thermal expansion coefficient was measured on bulk samples (DIL 404, Netzsch). The activation energies for crystallization (E_a) were calculated using Kissinger's equation[10,11] and DTA results with different heating rates (5, 10, 15 and 20 °C/min). Heat treatments were performed on bulk CZS samples in an electric kiln, (10 °C/min heating rate, isotherms at 1050 °C for 5, 15, 30 and 60 min and at 1150 °C for 30 min, slow cooling). Heat-treated bulk samples were subjected to scanning electron microscopy (SEM, XL-30, Philips) and XRD to better assess the crystalline phases formation.

Coatings were plasma-sprayed at Centro Sviluppo Materiali S.p.A. (Castel Romano, Italy) using a Sulzer-Metco F4-MB torch in a controlled atmosphere plasma spray (CAPS, co-shared with University La Sapienza, Roma) plant run in APS mode, with operating parameters listed in Table 1. Industrially manufactured porcelainized stoneware tiles and porous tile bodies and were employed as substrates; they were grit blasted with 500 μm alumina grits (Sulzer-Metco Metcolite-C) before deposition.

To achieve densification and crystallization of sprayed coatings, the following heat treatments were performed:

1. 15 °C/min heating to 850 °C, 30 min isotherm, 15 °C/min heating to 950 °C, 30 or 60 min isotherm, slow cooling; these treatments shall be referred to as 9–30 or 9–60, respectively;
2. 15 °C/min heating to 850 °C, 30 min isotherm, 15 °C/min heating to 1050 °C, 15 min (only for CZS) or 30 min isotherm, slow cooling; these treatments shall be referred to as 10–15 or 10–30, respectively.

As-sprayed and heat-treated coatings microstructures have been assessed by SEM (as-sprayed and polished surface, cross-section) and XRD. The diffraction patterns have been acquired also on ground samples (100 μm has been removed with SiC abrasive papers) to check the depth of the crystallization along the coating thickness. Measured mechanical properties include Vickers microhardness on polished surface and cross-section (HX-1000 indenter, Remet), indentation fracture toughness (using high-load Vickers indentations, measuring the cracks lengths through SEM and employing the Lankford formula in the calculations[12]), elastic modulus (four-points bending test, Z010 testing machine, Zwick/Roell) and deep abrasion resistance according to EN 10545.6 norm (AP/87 abrasimeter, Ceramic Instruments). The latter is an abrasion test were a flux of alumina particles with mean diameter around 180 μm falls tangentially to a rotating steel disk, pressed by a fixed load against the tested surface; the results are expressed as the ratio between the wear volume, in cubic millimetres, and the sliding distance, in metres). Acid resistance tests (4 days contact with HCl 18%, visual inspection and methylene blue treatment) have also been performed. Porcelainized stoneware and high-performance traditional industrial glazes were also tested for reference. Vickers microhardness and fracture toughness were also measured on cast bulk CAS and CZS glass samples.

3. Results

The chemical analysis of the frits substantially confirm the nominal compositions.

From DTA curves, it follows that CZS has $T_g \approx 780$ °C and crystallizes at about 1050 °C (the exact temperature slightly changes with the heating rate; Fig. 1A), forming wollastonite-2 M, $Ca_2ZrSi_4O_{12}$, and minor amount of larnite and baghda-

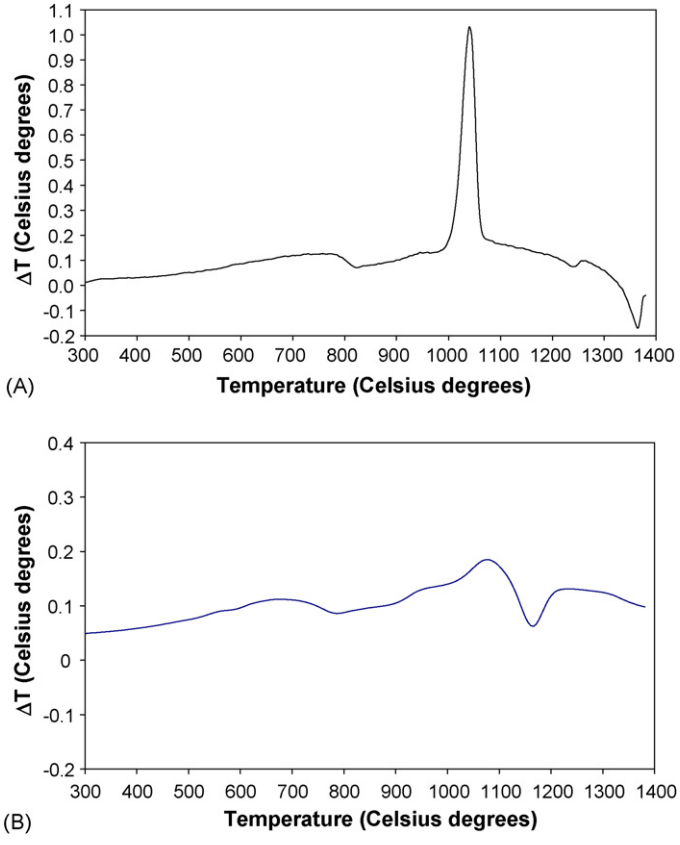

Fig. 1. DTA-curves of CZS frit (A) and CAS frit (B).

dite; two endothermal peaks around 1240 and 1360 °C probably reflect some phase transition or melting. CAS has $T_g \approx 760$ °C, a weak exothermal peak at about 1120 °C and an endothermal one at about 1170 °C (Fig. 1B). CZS has $E_a = 457$ kJ/mol, while $E_a = 507$ kJ/mol for CAS. The values for CZS are coherent with those reported for similar glass compositions,[10] where it has been found to decrease with addition of network modifiers. The crystallization process is usually controlled by long-range diffusion, which is easier in glasses where network modifiers weaken the three-dimensional network. Since the present CZS system does not contain significant amounts of modifiers, the diffusion process is difficult, explaining the high activation energy value. The smaller DTA exothermal crystallization peak and the higher E_a for CAS glass indicates that it has lower tendency to crystallization than CZS.

An almost complete surface crystallization is achieved on the surface of CZS bulk samples after heat treatment (Fig. 2A), but the cross-sectional depth of the crystallized surface layer is only a few microns, with a maximum of 50 μm after the 1150 °C for 30 min treatment (Fig. 2B). In particular, the many small $Ca_2ZrSi_4O_{12}$ crystals, which tend to cluster on the surface, extend only to a very limited depth (generally not higher than a few microns), while dendritic wollastonite crystals extend to a higher depth. These observations clearly indicate that the CZS system has a superficial crystallization. Very long treatment times would be necessary to develop a fully crystalline bulk CZS glass-ceramic.

The linear thermal expansion coefficients (100 °C < T < 500 °C) of the CZS and CAS systems are 7.48×10^{-6} and 6.81×10^{-6} °C^{-1}, respectively; for porcelainized stoneware and porous bodies, they are 8.49×10^{-6} °C^{-1} (100 °C < T < 600 °C) and 7.94×10^{-6} °C^{-1} (383 °C < T < 823 °C), respectively. Both frits cannot therefore be employed as the only constituent of a glaze if it is to be applied by above described conventional techniques, as they would develop unacceptable compressive residual stress which would plastically deform the tile during cooling and crack the coating itself.

According to laser granulometry, in the 20–100 μm range are included the 50% of CZS frit and the 54% of CAS frit, with the latter being slightly coarser. The particle size distribution is therefore suitable for plasma-spraying, even tough it is quite broad, which is undesirable for spraying parameters optimization.[13] The milling and classification operations would thus need a specific optimization research.

The as-sprayed CZS coating (Fig. 3A) has 11.4% average porosity (image analysis), which is quite high, but not too different from literature porosity values for plasma-sprayed coatings.[14] The CAS as-sprayed one (Fig. 3B) is more defective. Both the coatings show a broad band in the diffraction patterns, with no detected crystalline phase peaks (Fig. 4A and B, pattern a). They both present the lamellar microstructure of plasma-

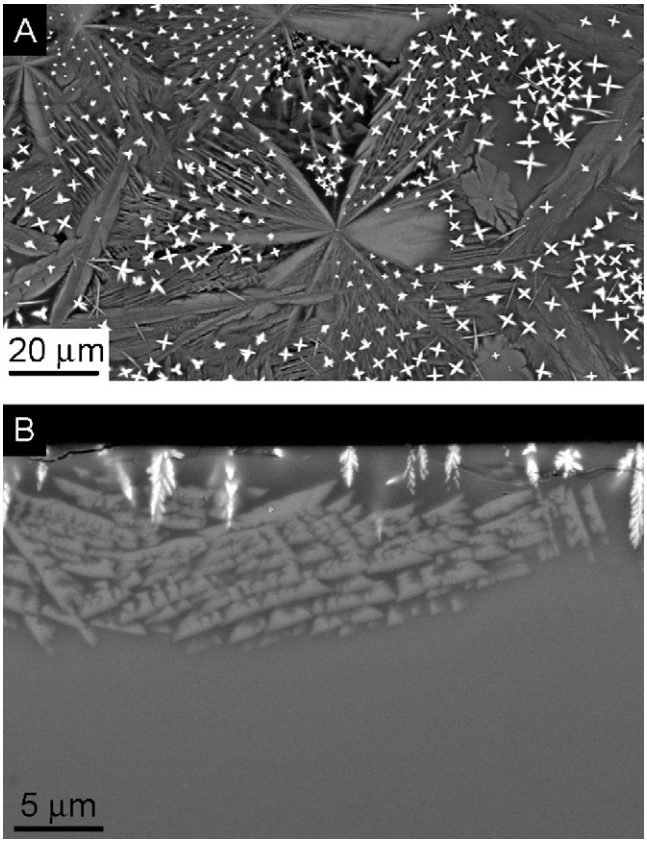

Fig. 2. SEM micrographs of the surface (A) of bulk CZS glass treated at 1050 °C for 60 min and cross-section (B) bulk CZS glass treated at 1150 °C for 30 min.

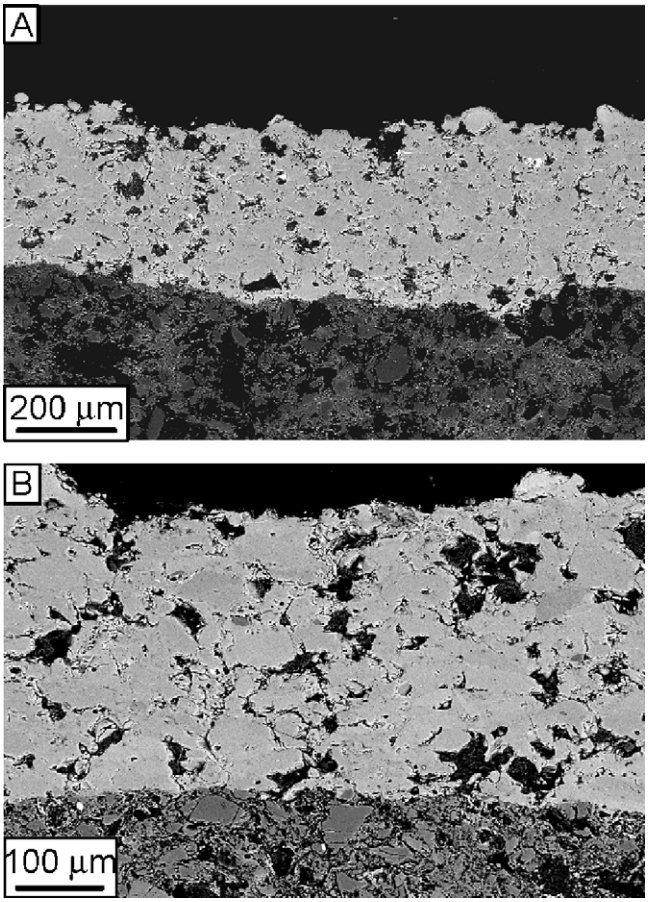

Fig. 3. Cross-section of as-sprayed CZS (A) and CAS (B) coatings on porous tile bodies.

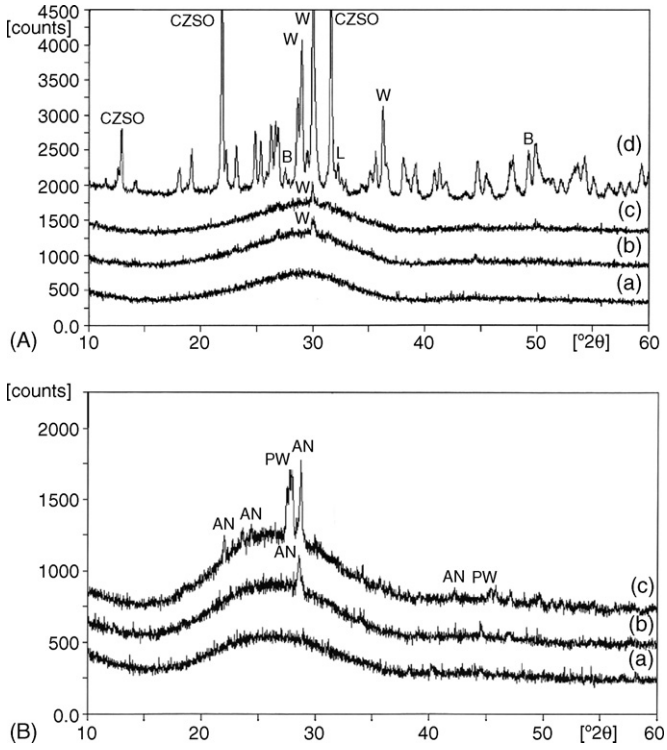

Fig. 4. XRD patterns of the plasma-sprayed coatings. All the examined coatings had ground surfaces. For sake of clarity, the labelling of the peaks concerns just the main ones of the different crystalline phases. (A) CZS coatings in the as-sprayed condition (a), after 850 °C for 30 min + 950 °C for 30 min (b), 850 °C for 30 min + 950 °C for 60 min (c) and 850 °C for 30 min + 1050 °C for 30 min (d) thermal treatment; CZSO, $Ca_2ZrSi_4O_{12}$; W, wollastonite-2 M ($CaSiO_3$); L, larnite (β-Ca_2SiO_4); B, baghdadite ($Ca_3ZrSi_2O_9$). (B) CAS coatings in the as-sprayed condition (a), after 850 °C for 30 min + 950 °C for 30 min (b) and 850 °C for 30 min + 1050 °C for 30 min (c) thermal treatment; AN, anortite ($CaAl_2Si_2O_8$); PW, pseudowollastonite (α-$CaSiO_3$).

sprayed coatings. White areas at the splat boundaries are a glassy phase richer in Ca and Zr. Notwithstanding the flaws of the coating, the interface with the substrate has low defectiveness. The defectiveness of as-sprayed coatings might be ascribed to different reasons: the broad particle size distribution, the low thermal conductivity of glasses which hinders heating and melting of the middle region of sprayed particles, the low density of glasses when compared to other engineering ceramics usually employed in thermal spraying (like alumina and zirconia) resulting in lower particle speed (the particle density affects the viscous drag) and lower kinetic energy upon impact. The higher defectiveness of CAS as-sprayed coatings is partly due to the difference between the two glass compositions (different density and viscosity of molten droplets), but mainly to the different grain size distribution of the CAS starting powders: the effect of increasing particle size distribution on higher porosity of plasma-sprayed coatings (mainly because of increased amount of unmolten material) has been widely discussed in literature.[13] The coatings defectiveness results in insufficient cohesion, thus causing low hardness and elastic modulus as compared to the corresponding bulk glass samples, and also low fracture toughness, with splat boundaries as preferential crack propagation paths (Table 2). Thus, wear mainly occurs by brittle splats removal along splat boundaries, consistently with literature data on other materials.[15] Acid resistance is not particularly good in as-sprayed coatings too, because the high defectiveness causes a high overall exposed surface area.

CZS and CAS 9–30 (Fig. 5A and B) and 9–60 samples show optimal sintering and adhesion to the substrate, but insignificant crystallization (Fig. 4A and B). Cohesion is enhanced, increasing Vickers microhardness and fracture toughness, but not up to the values of bulk glasses, which, being almost completely free of pores, represent the highest possible cohesion for these systems. Abrasion resistance increases, approaching or overcoming the best glazes (Table 2). The wear damage is now mainly due to brittle cracks propagation across the glass; the splat-like microstructure being lost.

CZS 10–30 and 10–15 samples (Fig. 6A) are considerably sintered (5% porosity from image analysis) and almost completely crystallized. X-ray diffraction peaks of the crystalline phases definitely prevail over the broad glassy band both on as-treated coatings surface and on ground surface (Fig. 4A, pattern d), suggesting that all of the coating thickness is equally crystallized, as SEM images show. In particular, from SEM

Table 2
Mechanical properties of tested materials

Material	Vickers microhardness, H_V (kg/mm^2)	Fracture toughness, K_{Ic} (MPa m$^{1/2}$)	Normalized wear volume, V_n (mm^3/m)	Elastic modulus, E (GPa)
Porcelainized stoneware	420 ± 46 (25)	1.628 ± 0.475	1.552	72
Industrial glaze	415 ± 48 (25)	–	2.080	–
As-sprayed CZS	457 ± 82 (25) (cross-section)	0.371 ± 0.217	3.198	31
9–30 CZS	511 ± 78 (25) (cross-section)	1.112 ± 0.141	2.390	–
9–60 CZS	498 ± 44 (25) (cross-section)	0.900 ± 0.165	1.540	–
10–30 CZS	622 ± 99 (50) (cross-section)	2.144 ± 0.446	1.194	110
10–15 CZS	594 ± 85 (50) (cross-section)	2.535 ± 0.623	0.720	–
Bulk CZS glass	575 ± 40 (25)	1.584 ± 0.216	–	95
Bulk CZS annealed glass	640 ± 63 (50)	Not measurable (layer too thin)		–
As-sprayed CAS	401 ± 68 (10) (cross-section)	Not measurable (too defective)	5.044	–
9–30 CAS	451 ± 63 (25) (cross-section)	1.123 ± 0.146	1.898	–
10–30 CAS	–	–	1.612	–
Bulk CAS glass	515 ± 66 (25)	1.711 ± 0.154	–	84

Microhardness indentation load is indicated in parenthesis.

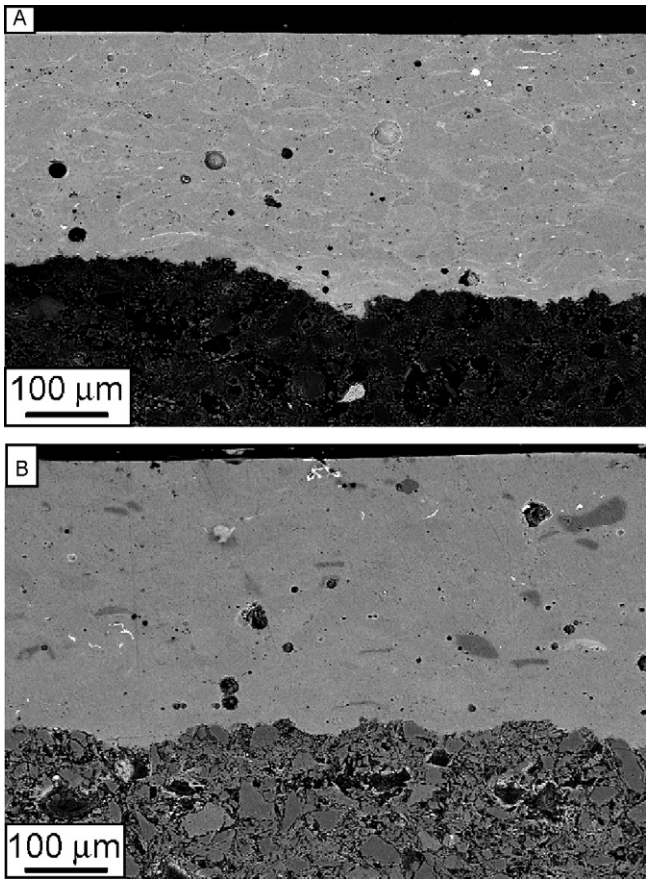

Fig. 5. Cross-section of CZS (A) and CAS (B) coatings on porous tile bodies, thermally treated at 850 °C for 30 min + 950 °C for 30 min.

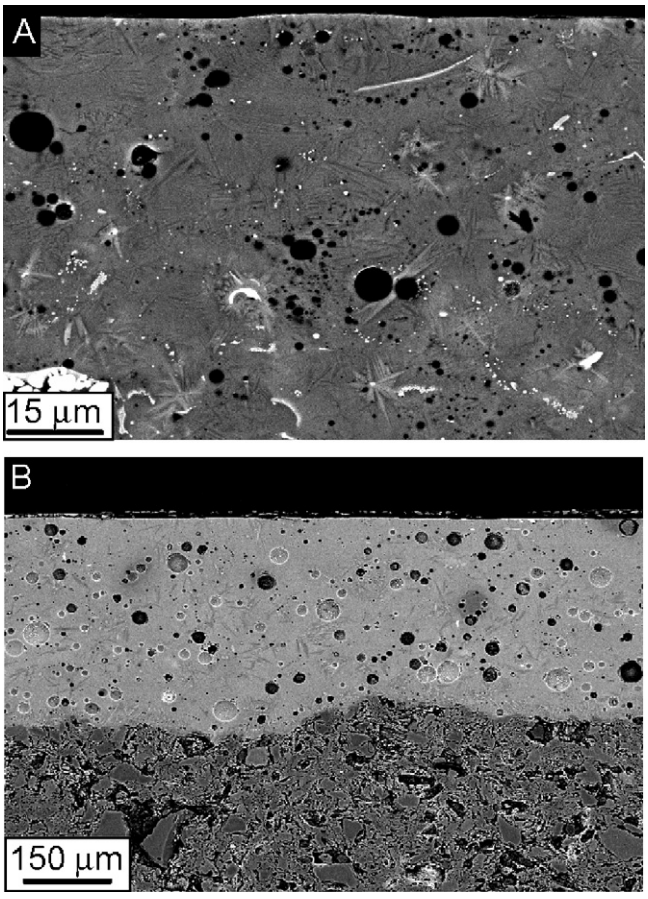

Fig. 6. Cross-section of CZS (A) and CAS (B) coatings on porous tile bodies, thermally treated at 850 °C for 30 min + 1050 °C for 30 min.

images, many groups of very small (≤1 μm) white crystals in a dendritic darker matrix are found; by EDS and XRD results they are $Ca_2ZrSi_4O_{12}$ and wollastonite-2 M, respectively. Crystal size is smaller in the 10–15 coating. The interface with the substrate is excellent, because, during the sintering stage, the glass infiltrates the substrate porosities, and, at higher temperature, crystals grow from the interface itself. The surprisingly high crystallinity degree of 10–30 and 10–15 CZS coatings when compared to bulk heat-treated CZS is probably caused by the many preferential surface nucleation sites represented by defects and substrate interface. Moreover, splat boundaries have developed a similar composition to $Ca_2ZrSi_4O_{12}$, probably because a slight glass phase separation takes place within molten droplets during plasma-spraying; they probably enhance the splat boundaries effect as preferential nucleation sites. As a consequence of the large crystallization, a definite increase in H_V (approaching heat-treated bulk CZS surface), E (very high for such glass-ceramics) and K_{Ic} (higher than bulk CZS glass and porcelainized stoneware) is found, indicating full exploitation of CZS capabilities. Higher K_{Ic} explains the better abrasion resistance than porcelainized stoneware; frequent crack deflections due to several small crystals is the microstructural reason for toughening. The higher number of smaller grains in 10–15 CZS coating causes more deflections, thus maximizing wear resistance. Unfortunately, 10–30 and 10–15 CZS coatings do not have optimal chemical resistance, a selective attack on wollastonite being clearly perceivable from SEM micrographs: this is an intrinsic limit of the present glass-ceramic composition, which can be overcome employing a different system, developing more acid-resistant phases. It must be considered that some colour difference is also noticed on porcelainized stoneware (generally regarded as the most chemically resistant among traditional ceramic tile materials) after methylene blue treatment.

CAS 10–30 coating (Fig. 6B) has formed some anorthite and pseudowollastonite, but is still mainly glassy (Fig. 4B, pattern c). This crystallization has also blocked sintering, so, a quite high porosity is found. Therefore, mechanical properties are not significantly enhanced.

4. Conclusions

High resistance coatings on ceramic substrates can actually be manufactured by plasma-spraying. Suitable post-process thermal treatments are needed; if they are correctly performed, the coating micromechanical properties and abrasion resistance definitely overcome the best industrial glazes and of unglazed porcelainized stoneware. The properties enhancement achieved after the thermal treatment is due to cohesion enhancement because of sintering and to toughening because of complete crystallization. The latter occurs thanks to the peculiar, splat-like,

defective microstructure of plasma-sprayed coatings providing preferential sites for nucleation, especially if surface nucleating systems (like the CZS one) are considered. Bulk CZS samples, where no other nucleation site exists except the surface itself, have a much slower crystallization kinetic, as confirmed by the high crystallization activation energy, and do not fully devitrify. The CAS glass is intrinsically unable to fully crystallize (small DTA crystallization peak and very high crystallization activation energy); thus, coatings remain mostly glassy. The thermal treatment can improve cohesion, but no toughening is therefore possible; so, mechanical properties cannot reach crystallized CZS levels. This indicates that the employment of glass-ceramics is preferable for mechanical properties optimization.

Acknowledgements

The authors are grateful to Centro Sviluppo Materiali S.p.A. (Castel Romano, Roma, Italy), and in particular to Ing. Fabrizio Casadei, Mr. Edoardo Severini and Mr. Valerio Ferretti, for performing the plasma spray runs, and to Prof. Teodoro Valente and his research group (Università di Roma, 1 La Sapienza) for the help with four-point bending tests. Frits and glazed tiles supplying by Colorobbia S.p.A. are acknowledged. Partially supported by PRRIITT (Regione Emilia Romagna), Net-Lab "Surface & Coatings for Advanced Mechanics and Nanomechanics" (SUP&RMAN).

References

1. Emiliani, G. P. and Corbara, F., *Tecnologia Ceramica – Vol. II: La Lavorazione*. Gruppo Editoriale Faenza Editrice, Faenza, 1999, pp. 383–441.
2. Herman, H., Sampath, S. and McCune, R., Thermal spray: current status and future trends. In *Thermal Spray Processing of Materials*, ed. S. Sampath and R. McCune. MRS Bullettin, July 2000, pp. 17–25.
3. Dorfman, M. R., Thermal spray applications. *Advanced Materials and Processes*, 2002, **160**(10), 66–68.
4. Vardelle, A., Fauchais, P., Dussoubs, B. and Themelis, N. J., Heat generation and particle injection in a thermal plasma torch. *Plasma Chemistry and Plasma Processing*, 1998, **18**, 551–572.
5. Bessmertnyi, V. S., Krokhin, V. P., Panasenko, V. A., Drizhd, N. A., Dyumina, P. S. and Kolchina, O. M., Plasma rod decorating of household glass. *Glass and Ceramics*, 2001, **58**, 214–215.
6. Gawne, D. T., Qiu, Z., Bao, Y., Zhang, T. and Zhang, K., Abrasive wear resistance of plasma-sprayed glass-composite coatings. *Journal of Thermal Spray Technology*, 2001, **10**(4), 599–603.
7. Weaver, D. T., Van Aken, D. C. and Smith, J. D., The role of bulk nucleation in the formation of crystalline cordierite coatings produced by air plasma spraying. *Materials Science and Engineering A*, 2003, **339**, 96–102.
8. Schrooten, J. and Helsen, J. A., Adhesion of bioactive glass coating to Ti6Al4V oral implant. *Biomaterials*, 2000, **21**, 1461–1469.
9. Gabbi, C., Cacchioli, A., Locardi, B. and Guadagnino, E., Bioactive glass coating: physicochemical aspects and biological findings. *Biomaterials*, 1995, **16**, 515–520.
10. Ferrari, A. M., Leonelli, C., Pellacani, G. C. and Siligardi, C., Effect of V_2O_5 addition on the crystallisation of glasses belonging to the $CaO–ZrO_2–SiO_2$ system. *Journal of Non-Crystalline Solids*, 2003, **315**, 77–88.
11. Ray, C. S. and Day, D. E., Nucleation and crystallization in glasses as determined by DTA. *Ceramic Transactions*, 1993, **30**, 207–223.
12. Lankford, J., Twinning and microcrack nucleation during indentation of aluminum oxide. *Scripta Metallurgica*, 1977, **11**, 349–351.
13. Ang, C. B., Devasenapathi, A., Ng, H. W., Yu, S. C. M. and Lam, Y. C., A proposed process control chart for DC plasma spraying process. Part II. Experimental verification for spraying alumina. *Plasma Chemistry and Plasma Processing*, 2001, **21**, 401–419.
14. Wang, Z., Kulkarni, A., Deshpande, S., Nakamura, T. and Herman, H., Effects of pores and interfaces on effective properties of plasma sprayed zirconia coatings. *Acta Materialia*, 2003, **51**, 5319–5334.
15. Westergärd, R., Erickson, L. C., Axén, N., Hawthorne, H. M. and Hogmark, S., The erosion and abrasion characteristics of alumina coatings plasma sprayed under different spraying conditions. *Tribology International*, 1998, **31**, 271–279.